Advance in the Dynamics and Targeted Observations of Tropical Cyclone Movement

Chun-Chieh Wu
Department of Atmospheric Sciences, National Taiwan University, Taipei, Taiwan
cwu@typhoon.as.ntu.edu.tw

The advance in the dynamics and targeted observations of hurricane movement is reviewed in this article. In celebration of the 50th anniversary of the Department of Atmospheric Sciences, National Taiwan University, special emphasis is put on the author's major scientific contributions to the following issues: the baroclinic effect on tropical cyclone motion, the potential vorticity diagnosis of the tropical cyclone motion, and the targeted observations from DOTSTAR (Dropwindsonde Observations for Typhoon Surveillance near the Taiwan Region) in understanding and improving the tropical cyclone track predictability.

1. Introduction

The dynamics of tropical cyclone (TC) motion are rather complex. As pointed out by Holland (1984), a complete description would require at least detailed knowledge of the interactions between the cyclone circulation, the environmental wind field, the underlying surface, and the distribution of moist convection. It has generally been proposed that TC motion is governed by the tropospheric average steering flow and a drift caused by the presence of a background potential vorticity gradient. However, there are many other factors that can affect the cyclone's motion. Thanks to scientific advances in the past few decades, the understanding of the dynamics of TC motion is rather comprehensive, along with the improvement of observations (Aberson, 2003; Wu *et al.*, 2005) and numerical models (Kurihara *et al.*, 1998); the forecasting of TC motion has also been in steady progress.

Some reviews on this issue have been well conducted, by Wang *et al.* (1998) and Chan (2005). To celebrate the 50th anniversary of the Department of Atmospheric Sciences, National Taiwan University, this article reviews the author's major contributions to the current understanding of the dynamics and targeted observations of TC movement. The following topics are covered: the baroclinic effect on TC motion (Wu and Emanuel, 1993, 1994), the potential vorticity perspective of the TC motion (Wu and Emanuel, 1995a,b; Wu and Kurihara, 1996; Wu *et al.*, 2003, 2004), and the targeted observations in improving TC track prediction (Wu *et al.*, 2005, 2006, 2007a,b). In Sec. 2, the baroclinic effect on TC motion is shown. The potential vorticity perspective of the TC motion and the targeted observations from DOTSTAR (Dropwindsonde Observations for Typhoon Surveillance near the Taiwan Region) in improving the forecasting of TC motion are discussed in Secs. 3 and 4, respectively. Finally, a summary appears in Sec. 5.

2. Baroclinic Effect on TC Motion (Wu and Emanuel, 1993, 1994)

2.1. *Background*

Studies of TC motion have focused mainly on steering by the mean flow and the effect of background potential vorticity gradients, i.e. the evolution of barotropic vortices in a barotropic flow. These effects, taken together, suggest that TCs should follow the mean large scale (steering) flow (George and Gray, 1976), but with a westward and poleward relative drift (Fiorino and Elsberry, 1989). Other, minor factors may also affect TC motion, such as the asymmetric convection (Willoughby, 1988) and the vortex interaction (Holland and Dietachmayer, 1993).

However, observations have shown that real TCs are strongly baroclinic, with broad anticyclones aloft, and the distribution of the large-scale potential vorticity gradient in the tropical atmosphere is very nonuniform. As indicated by Wu and Emanuel (1993), these properties may substantially influence the movement of storms. The upper anticyclone, though weak in terms of wind velocity relative to the lower-layer cyclonic circulation, can be very extensive. Slight displacements of the upper region of anticyclonic flow from the low-level cyclone can conceivably lead to large mutual interaction, and the potential vorticity gradient may act on these two flows in very different ways.

Based on the concepts of vortex interaction, Wu and Emanuel (1993) proposed that a baroclinic TC, which is structured like a vertically distributed pair of vortices of opposite signs, would experience a mutual propagation if the vortex dipole is tilted (Fig. 1). In other words, the background vertical wind shear can tilt the vortex pair by blowing the upper potential vorticity anomaly downshear. As members of the vortex pair are displaced, they begin to interact with each other and thus move at right angles to the axis connecting them. On this basis, it is hypothesized that Northern Hemispheric (Southern Hemispheric) TCs should drift with respect to the mean winds in a direction to the left (right) of the background vertical shear vector.

2.2. *Methodology*

The intention is to isolate the effect of background vertical shear. The hurricane is represented in a two-layer quasi-geostrophic model as a point source of mass and zero potential vorticity air in the upper layer, collocated with a point cyclone in the lower layer. The model is integrated by the method of contour dynamics and contour surgery. The contour dynamics is a

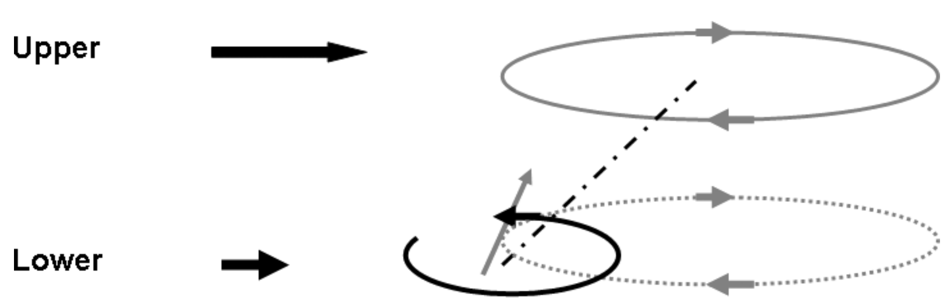

Figure 1. The vertical shear (black arrows) of the environmental flow results differential advection of the potential vorticity associated with a storm. Black and gray ellipses indicate the lower- and upper-level storm circulations, respectively. The upper layer is tilted due to the presence of vertical shear, and its projection (dashed gray ellipse) results in the storm drift to the left (Northern Hemisphere) of the shear vector (gray arrow).

Lagrangian computational method used to integrate flows associated with patches of piecewise constant potential vorticity. This method leads to a closed dynamical system within which the evolution of the flow can be uniquely determined by the contours bounding the patches. The method of contour surgery improves the resolution of the contour by adding nodes (called node adjustment) in regions of high curvature or small node velocity. It is also more efficient and prevents unlimited enstrophy cascades to a small scale by removing contour features (called contour adjustment) thinner than some prescribed tolerance. A detailed description of the methods of contour dynamics and contour surgery can be found in Dritschel (1989).

In this work, the simplest analog of a mature TC is considered to be a diabatically, frictionally maintained point vortex of constant strength in the lower layer, and a patch of uniform, zero potential vorticity air in the upper layer, surrounded by an infinite region of constant potential vorticity (it is assumed that the mean meridional gradient of potential vorticity associated with the coriolis parameter can be canceled out by introducing upper and lower boundaries with gentle meridional slopes in the two-layer model). The diabatic sink of potential vorticity in the upper layer is represented as the expansion of the upper potential vorticity anomaly, owing to a radial outward potential (irrotational) flow emanating from a point mass source collocated with the lower vortex. According to the principle of mass continuity, the potential flow can be calculated from the lower boundary frictionally driven mass influx.

The case of a vanishing ambient potential vorticity gradient is explored as well. Therefore, the upper vortex patch is advected by the rotational flows (associated with both the upper-layer contour itself and the lower-layer vortex), the divergent flow (associated with the mass source), and the mean shear flow. The work of Wu and Emanuel (1993, 1994) is meant to describe the first-order effects of vertical shear, given the approximation inherent in the model.

2.3. *Results*

For the case with no vertical shear, it is found that, as expected, the upper patch expands with time and remains circularly symmetric with no lower vortex movement. The wind distributions in each layer show that the upper flow is anticyclonic and outward, similar to a real hurricane outflow, and the lower layer flow is symmetric around the vortex center, so that no vortex drift is induced.

For the case with shear, the vortex patch expands and is advected downshear. Also, roll-up of the vortex patch occurs on the downshear side, essentially due to barotropic instability. For cases with larger shear, the patch is advected rapidly downshear and becomes zonally elongated. The low potential vorticity anomaly behaves like a passive plume.

The trajectories of the lower vortex in three experiments with westerly shear of various magnitudes are shown in Fig. 2. In all cases,

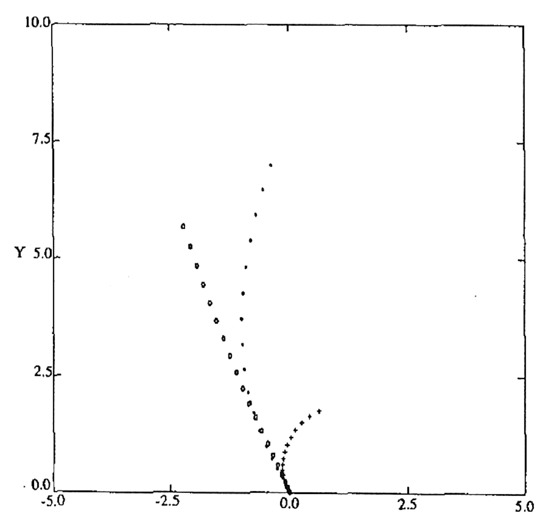

Figure 2. Trajectories (units of 500 km) of the lower-layer vortex encountering weaker (shown as +); fair (shown as ∗); and stronger (shown as ∘) vertical wind shear. (From Wu and Emanuel, 1993).

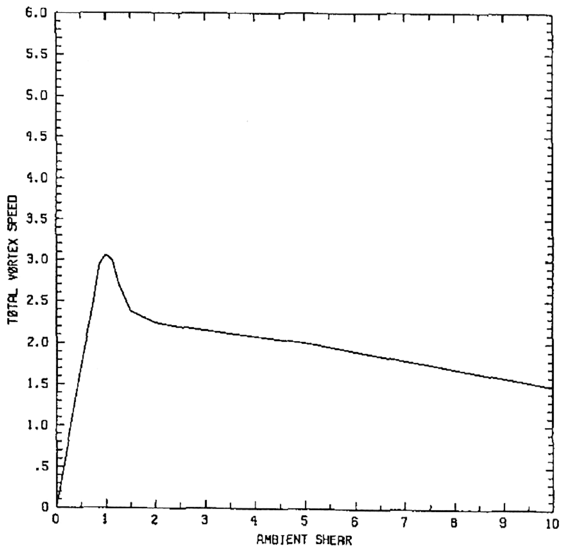

Figure 3. The relation between the maximum induced vortex speed and the magnitude of the vertical shears. (From Wu and Emanuel, 1993.)

distinct northward vortex drifts associated with different magnitudes of the mean westerly shears are found, as expected. Also, the drift in the zonal direction is a function of the background shear, i.e. more eastward drift is associated with weaker shear. Figure 3 shows the maximum total drift speed as a function of the ambient shear. The vortex drift increases initially as the shear increases, and there exists an optimal shear that maximizes the vortex drift. Above that optimal shear, the drift speed decreases with increasing shear, and approaches a constant, since the impact to the lower-layer vortex drift by the upper-layer plumed advected far downstream would be very limited.

2.4. *Summary*

Observations show that TCs have broad anticyclones aloft, and that the distribution of potential vorticity gradients in the tropical atmosphere is highly inhomogeneous. There are indications that the potential vorticity gradients in the subtropical troposphere are very weak (see Fig. 2 in Wu and Emanuel, 1993), perhaps having been rendered so by the action of synoptic scale disturbances.

It is found that the direct effect of ambient vertical shear is to displace the upper-level plume of anticyclonic relative potential vorticity downshear from the lower layer cyclonic point potential vortex, thus inducing a mutual interaction between the circulations associated with each other. This results in a drift of the point vortex broadly to the left of the vertical shear vector (in the Northern Hemisphere).

3. Potential Vorticity Perspective of TC Motion (Wu and Emanuel, 1995a,b; Wu and Kurihara, 1996; Wu *et al.*, 2003, 2004)

The above papers are some pioneering works in adopting the potential vorticity (PV) diagnostics to evaluate the control by the large-scale environment of hurricane movement and, more importantly, to assess the storm's influence on its own track. By using the PV framework, the exploration of the dynamics of hurricanes is feasible with the validity of balanced dynamics in the tropics. In this section, the use of PV diagnostics is to understand the hurricane steering flow, and to demonstrate the interaction between the cyclone and its environment, including the investigation of the binary TC interaction and the major factors affecting the analyses and forecast bias of the TC track forecasts.

3.1. *Background*

PV methods have proven useful in understanding synoptic- and large-scale midlatitude dynamics (Hoskins *et al.*, 1985), and are widely applied to tropical systems (e.g. Molinari, 1993; Montgomery and Farrell, 1993). A hurricane is a localized yet robust vortex, and can possibly change the surrounding environmental flow field substantially by its strong circulation, which in turn affects the evolution of the track, intensity, and structure of the hurricane. This interaction between the TC and its environment is nonlinear. Previous studies have investigated how the large-scale flow fields affect the track, intensity (e.g. Molinari *et al.*, 1995), and structure of the hurricane, and how the storm circulation changes the environmental flow field (e.g. Ross and Kurihara, 1995). However, these studies consider only a one-way interaction between the storm and its environment. In this work, the two-way hurricane–environment interaction is studied, i.e. how the change of the environment due to the storm feeds back to affect the storm's track.

The concept of binary interaction has been well described by tank experiments (Fujiwhara, 1921, 1923, 1931), observations (Brand, 1970; Dong and Neumann, 1983; Lander and Holland, 1993; Carr *et al.*, 1997; Carr and Elsberry, 1998), and modeling studies (Chang, 1983, 1984; DeMaria and Chan, 1984; Ritchie and Holland, 1993; Holland and Dietachmayer, 1993; Wang and Holland, 1995). All of these studies indicate that two TCs can interact and subsequently develop mutual orbiting and possible approaching, merging, and escaping processes (Lander and Holland, 1993).

The observational evidences Brand (1970) has provided suggest that there is a correlation between the separation distance and the angular rotation rate of two TCs. Brand also showed that the effect of such binary interaction depends not only on differences in storm size and intensity, but also on variations of the currents in which the tropical storm systems are imbedded.

Work from Carr *et al.* (1997) and Carr and Elsberry (1998) has proposed detailed conceptual models to categorize the binary interaction processes, namely: (1) the direct TC interaction with one-way influence, mutual interaction or merger of the two TCs; (2) the semidirect TC interaction involving another TC and an adjacent subtropical anticyclone; and (3) the indirect TC interaction involving the anticyclone between the two TCs. In spite of a success rate of 80% in distinguishing the modes of the binary interactions from analyses of eight-year samples of western North Pacific TCs, the ways to quantify the binary interaction of TCs are still arguable.

This section has attempted to demonstrate the quantitative use of PV diagnostics in understanding the hurricane steering flow, in addition to the interaction between the cyclone and its environment, along with the binary TC interaction and the evaluation of the forecast bias.

3.2. *Methodology*

(1) *Defining the hurricane advection flow*
This is an original work to define the hurricane advection (steering) flow based on the PV diagnostics. One conventional problem in estimating the steering flow based on the azimuthal average is that the resulting wind is highly sensitive to the exact choice of the hurricane center (if the storm center is misrepresented, the averaged flow would be contaminated by the asymmetric high wind near and off the storm center). To avoid such a problem, the hurricane advection flow is defined as the balanced flow (at the storm center) associated with the entire PV field in the troposphere, except for the PV anomaly of the hurricane itself.

(2) *PV inversion*
The PV inversion is that given a distribution of PV, a prescribed balances condition, and boundary conditions, the balanced mass and wind fields can be recovered. Formulated on the $\pi\,[\pi = C_p(p/p_0)^\kappa]$ coordinate and spherical coordinates, the two equations to be solved are

$$q = \frac{gk\pi}{p}\left[(f + \nabla^2\Psi)\frac{\partial^2\Phi}{\partial\pi^2} - \frac{1}{a^2\cos^2\phi}\frac{\partial^2\Psi}{\partial\lambda\partial\pi} \times \frac{\partial^2\Phi}{\partial\lambda\partial\pi} - \frac{1}{a^2}\frac{\partial^2\Psi}{\partial\phi\partial\pi}\frac{\partial^2\Phi}{\partial\phi\partial\pi}\right], \qquad (1)$$

$$\nabla^2\Phi = \nabla\cdot(f\nabla\Psi) + \frac{2}{a^4\cos^2\phi} \times \frac{\partial(\partial\Psi/\partial\lambda, \partial\Psi/\partial\phi)}{\partial(\lambda,\phi)}, \quad (2)$$

where q represents PV, Φ represents geopotential height, and Ψ represents stream function, whereas a is the Earth's radius, f is the Coriolis parameter, $\kappa = R_d/C_p$, ϕ is longitude, and λ is latitude. Given the distribution of q, the lateral boundary of Φ and Ψ, along with θ on the upper and lower boundaries, the distribution of Φ and Ψ can be solved. Therefore, the nondivergent wind and potential temperature can also be obtained through the following two relations:

$$\vec{V} = \hat{k}\times\nabla\Psi, \quad (3)$$

$$\theta = -\frac{\partial\Phi}{\partial\pi}. \quad (4)$$

In the PV inversion method, another robust strength is the piecewise PV inversion, i.e. when the flow field is divided into the mean and perturbation components, the above equation can be rederived (Davis, 1992) to obtain the balanced fields associated with each individual PV perturbation. By taking the perturbation field as $\Psi' = \Psi - \bar{\Psi}$, $\Phi' = \Phi - \hat{\Phi}$, and $q' = q - \hat{q}$, the piecewise PV inversion is to calculate the balanced flow and mass fields associated with each PV perturbation. Such a method describes how the different PV features, the environment perturbations, affect the TC's track (Wu and Emanuel, 1995a,b; Shapiro, 1996; Shapiro and Franklin, 1999; Wu and Kurihara, 1996; Wu *et al.*, 2003, 2004).

(3) *Defining AT: the normalized steering effect associated with each PV perturbation in the along-track direction*

In order to evaluate the steering flow due to various PV perturbations, the time series of the deep-layer-mean (DLM) flow associated with the total PV perturbation $[\tilde{\mathbf{V}}_{\mathrm{SDLM}}(q')]$ and each PV perturbation $[\tilde{\mathbf{V}}_{\mathrm{SDLM}}(q'_a)]$ is defined. Note that $q' = q'_a + q'_{na}$ while the subscript "a" represents some specific perturbation of interest and "na" stands for the remaining perturbation. The DLM (925–300-hPa-averaged) steering wind is defined as

$$\vec{\mathbf{V}}_{\mathrm{SDLM}} = \frac{\int_{925\,\mathrm{hPa}}^{300\,\mathrm{hPa}} \vec{\mathbf{V}}_S(p)dp}{\int_{925\,\mathrm{hPa}}^{300\,\mathrm{hPa}} dp}, \quad (5)$$

where

$$\vec{\mathbf{V}}_S(p) = \frac{\int_0^3\int_0^{2\pi}\vec{\mathbf{V}}rdrd\theta}{\int_0^3\int_0^{2\pi}rdrd\theta}. \quad (6)$$

To realize the influence of the steering flow associated with each perturbation, the ratio of the steering flow associated with each perturbation to that associated with all perturbations has been calculated. Following Wu *et al.* (2003), this quantity is defined as

$$AT(q'_a) = \frac{|\vec{\mathbf{V}}_{\mathrm{SDLM}}(q'_a)\cdot\vec{\mathbf{V}}_{\mathrm{SDLM}}(q')|}{|\vec{\mathbf{V}}_{\mathrm{SDLM}}(q')|^2}, \quad (7)$$

where $\tilde{\mathbf{V}}_{\mathrm{SDLM}}(q'_a)$ and $\tilde{\mathbf{V}}_{\mathrm{SDLM}}(q')$ are as defined in Eq. (5). Note that by definition, $\mathrm{AT}(q') = \mathrm{AT}(q'_a) + \mathrm{AT}(q'_{na})$.

(4) *Defining the new centroid for plotting the centroid-relative track*

Conventionally, the centroid-relative tracks based on geography centers are often plotted to illustrate the binary interaction. This picture is often misleading, since the actual binary interaction is generally a function of the strengths of both vortices, and would not rotate with respect to the geographic center (Lander and Holland, 1993; Carr *et al.*, 1997; Carr and Elsberry, 1998; Wu *et al.*, 2003). In this article, the definition of the centroid from Wu *et al.* (2003) is discussed, i.e. the centroid between storms A and B is defined as the location weighted according to the strength of the steering flow induced by the PV perturbation associated with each storm:

$$\vec{\mathbf{r}}_c = \frac{|\vec{\mathbf{V}}_{\mathrm{SDLM}}(q'_A)|}{|\vec{\mathbf{V}}_{\mathrm{SDLM}}(q'_A)| + |\vec{\mathbf{V}}_{\mathrm{SDLM}}(q'_B)|}\vec{\mathbf{r}}_A + \frac{|\vec{\mathbf{V}}_{\mathrm{SDLM}}(q'_B)|}{|\vec{\mathbf{V}}_{\mathrm{SDLM}}(q'_A)| + |\vec{\mathbf{V}}_{\mathrm{SDLM}}(q'_B)|}\vec{\mathbf{r}}_B, \quad (8)$$

where $q'_A(q'_B)$ represents the perturbation PV of storm A (B), while $\vec{\mathbf{r}}_c$, $\vec{\mathbf{r}}_A$, and $\vec{\mathbf{r}}_B$ stand for the position vectors of the centroid, storm A, and storm B, respectively.

3.3. *Results*

(1) *PV diagnostics of the motion of Hurricane Bob (1991), Tropical Storm Ana (1991), and Hurricane Andrew (1992) (Wu and Emanuel, 1995a,b)*

In Wu and Emanuel (1993, 1994), the results of the advection flow of Bob show that Bob's movement is due not only to the climatological (July–September) mean balanced flow, but also to significant contributions from the balanced flow associated with the upper-tropospheric PV perturbations (U) [Fig. 4(a)]. This implies that Bob's motion is strongly influenced by the mid-latitude systems and the disturbances in the upper troposphere. However, in the case of Ana, the advection of this tropical storm is mainly associated with the mean flow and the PV perturbation in the lower troposphere. Unlike the case of Bob, due to the cancellation effects between the PV anomalies (i.e. the balanced flows associated with different pieces of the upper PV anomalies tend to aim toward different directions), the upper PV perturbation does not have a large effect on Ana's motion [Fig. 4(b)]. And for Hurricane Andrew, the climatological mean, upper and lower PV perturbations have about the same magnitude of contribution to the advection flow [Fig. 4(c)].

Compared to the annular mean winds, the analysis by Wu and Emanuel (1995a,b) provides a more dynamically consistent method of determining the advection flow through the hurricane center. In addition, the PV framework is conceptually more concise (Hoskins *et al.*, 1985), and allows one to study the essential dynamical mechanism responsible for hurricane motion.

(2) *A new look at the binary interaction: potential vorticity diagnosis of the unusual southward motion of Tropical Storm Bopha (2000) and its interaction with Supertyphoon Saomai (2000) (Wu et al., 2003)*

Tropical Storm Bopha (2000) showed a very unusual southward course parallel to the east coast of Taiwan, mainly steered by the circulation associated with Supertyphoon Saomai (2000) to Bopha's east.

To quantitatively measure the influence of the steering flow associated with other PV features in this binary interaction, the method shown in Subsec. 3.2(2) is adopted. Results show that the total PV perturbation provides

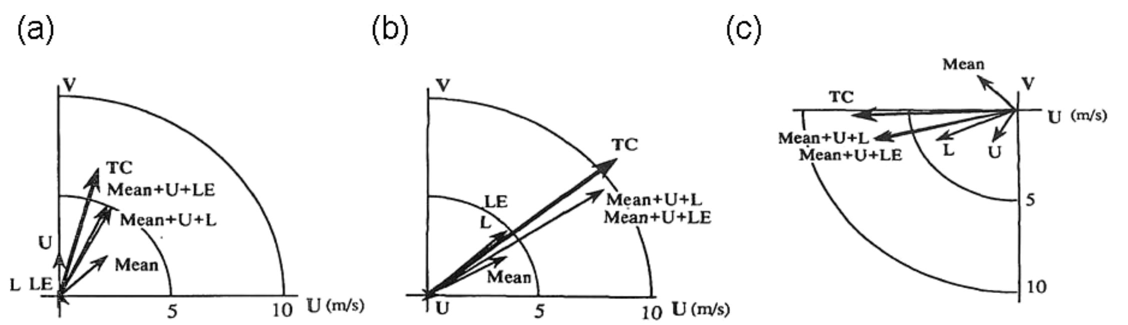

Figure 4. Interpolation of the balanced wind fields to the 850–500 mb pressure-averaged balanced vortex center. Mean, U, L, and LE represent the 850–500 mb pressure-averaged balanced flows associated with the mean potential vorticity, and potential vorticity perturbations of U, L, and LE, respectively. Mean + U + LE represents the total hurricane advection flow. TC indicates (a) Hurricane Bob's motion at 1200 UTC, 18 August 1991; (b) Tropical Storm Ana's motion at 1200 UTC, 3 July 1991; (c) Hurricane Andrew's motion at 1200 UTC, 23 August 1992. (From Wu and Emanuel, 1995a,b.)

a good approximation of the actual motion of both storms, Bopha and Saomai. Besides, Saomai plays the dominant role in advecting Bopha southward while the influence of Bopha on Saomai is rather limited (Fig. 5).

To better indicate the binary interaction processes, the new method for ploting the centroid-relatice track is devised. As shown in Fig. 6, Bopha and Saomai mutually interacted by rotating cyclonically around each other at a distance of about 1200 km, with the centroid much closer to Saomai. The unusual southward drift of Bopha appears to agree with the proposed mechanism as the direct binary interaction with one-way influence (Carr *et al.*, 1997). Clearly, the above PV analysis with the AT values can nicely quantify the binary interaction processes, and the newly defined centroid-relative track can describe the appropriate interaction of the TCs.

(3) *PV diagnosis of the key factors affecting the motion of Typhoon Sinlaku (2002) (Wu et al., 2004)*

Typhoons over the western North Pacific often move westward or northwestward due to the dominating steering flow associated with the Pacific Subtropical High (SH). However, forecasts of typhoons are sometimes difficult during the late season as typhoons approach about 130°E, where some storms may slow down, stall, or even recurve due to the weakening of the SH, as well as the strengthening of the Continental High (CH) over China and the presence of the deep midlatitude baroclinic wave or trough (TR). The stalling scenario appeared in the case of Sinlaku, where forecasts from some major operational centers failed to predict its slowdown and mistakenly predicted its southward dip before it approached the offshore northeastern Taiwan.

The PV diagnosis indicates that the initial deceleration of Sinlaku was mainly associated with the retreat of the SH under the influence of the TR. The upper-level cold-core low (CCL) played only a minor role in impeding Sinlaku from moving northward, while the CH over mainland China strongly steered Sinlaku westward. On account of the steering effects from the above four systems (SH, TR, CCL, and CH), which tend to cancel one another, the subtle interaction therein makes it difficult to make a precise track forecast (Fig. 7). This proposes another challenge to TC track forecasts in this region.

3.4. *Summary*

The validity of balance dynamics in the tropics allows us to explore the dynamics of hurricanes using the PV framework. Subsection 3.3 demonstrated the use of PV diagnostics in understanding the hurricane steering flow, and the interaction between the cyclone and its environment. The results are consistent with the previous finding that the hurricane advection flow, defined by inverting the entire PV distribution which excludes the storm's own positive anomaly, is a good approximation to real cyclone movement, even though the original data cannot capture the actual hurricane strength.

Moreover, the binary interaction between two typhoons is well demonstrated by the PV diagnosis. The quantitative description of the Fujiwhara effect is not easy for real-case TCs, because it tends to be masked by other environmental steering flows. A new centroid-relative track is proposed, with the position weighting based on the induced steering flow due to the PV anomaly of another storm. Such analysis is used to understand more complicated vortex merging and interacting processes between and among multiple TCs from either observational data or specifically designed numerical experiments. Finally, the PV inversion concept has been successfully applied to real-time analysis and prediction systems, and to quantitatively evaluate the factors affecting the storm motions.

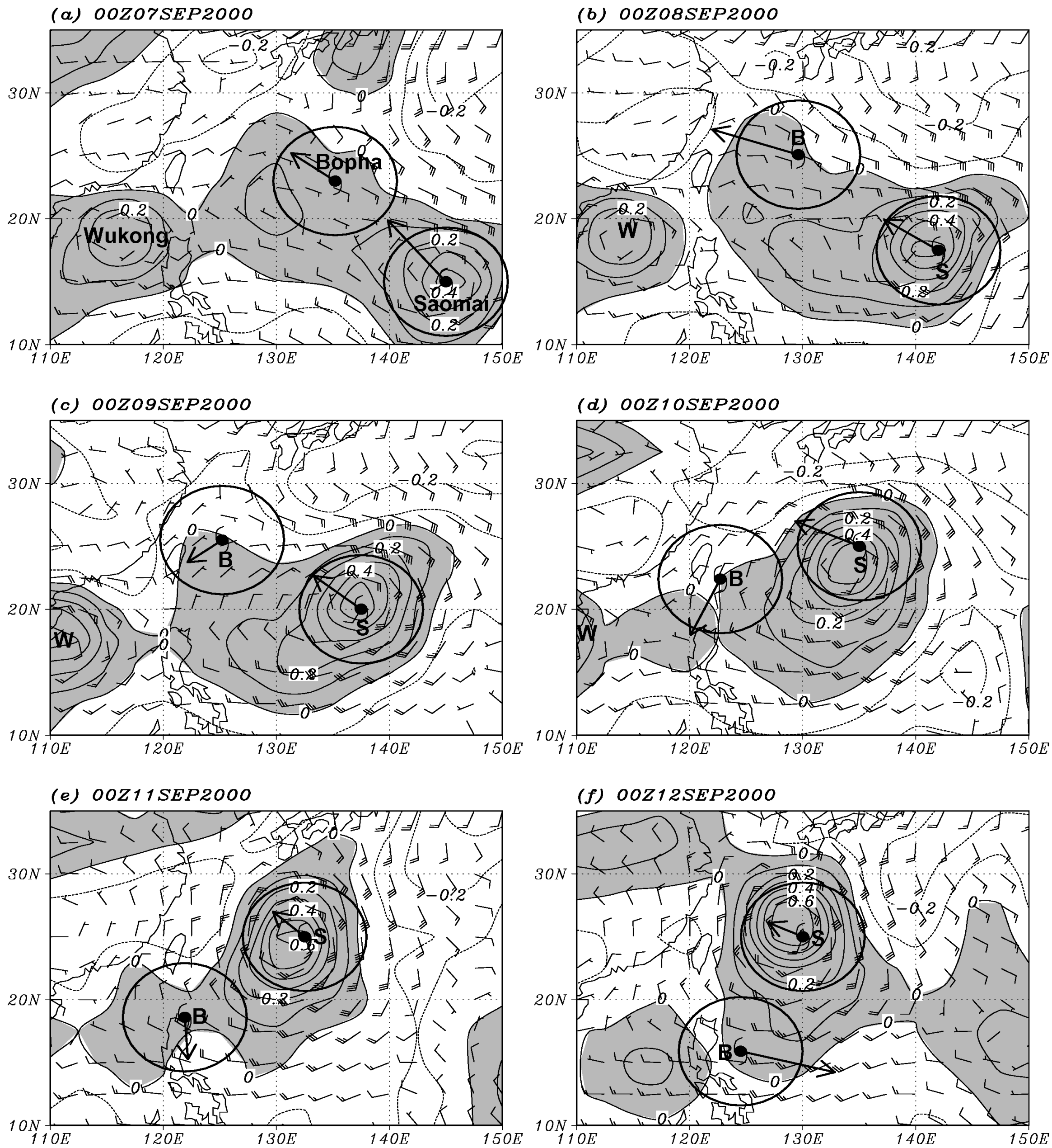

Figure 5. Total potential vorticity perturbation (contour interval of 0.1 PVU; the positive PV perturbation is shaded) at 500 hPa, and the 925–400 hPa deep-layer wind while Bopha is the mean part (one full wind barb = $5\,\mathrm{ms}^{-1}$) at 0000 UTC: (a) 7 September, (b) 8 September, (c) 9 September, (d) 10 September, (e) 11 September, and (f) 15 September 2000. The instantaneous movement of Bopha, as well as Saomai, is indicated by the bold arrow, whose length represents the actual translation velocity, and the sold circle shows the scale of $5\,\mathrm{ms}^{-1}$. B, S, and W indicate Bohpa, Saomai, and Wukong, respectively. (From Wu *et al.*, 2003.)

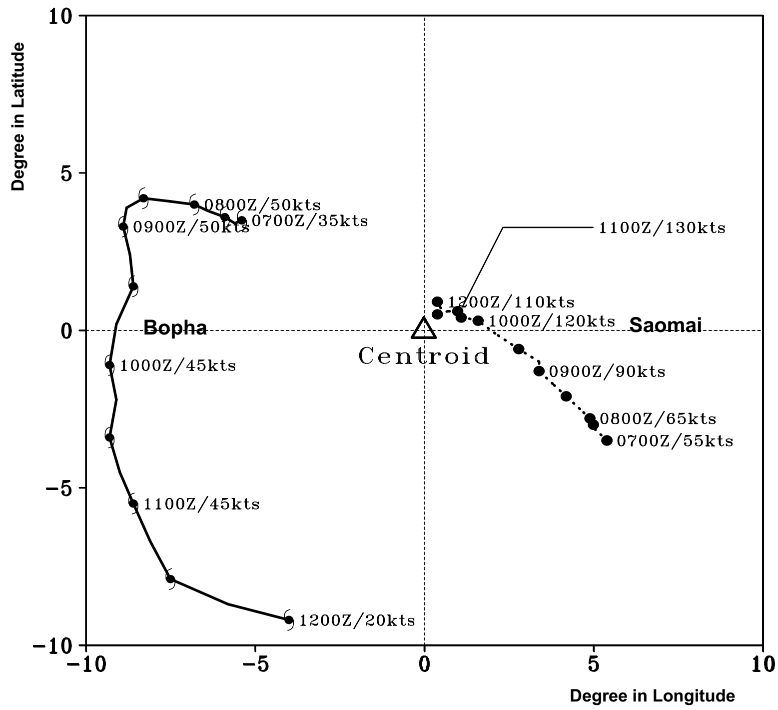

Figure 6. Centroid-relative tracks of Bopha (TC symbol) and Saomai (solid dot) for every 12 h from 0000 UTC, 7 September, to 0000 UTC, 12 September 2000. (From Wu *et al.*, 2003.)

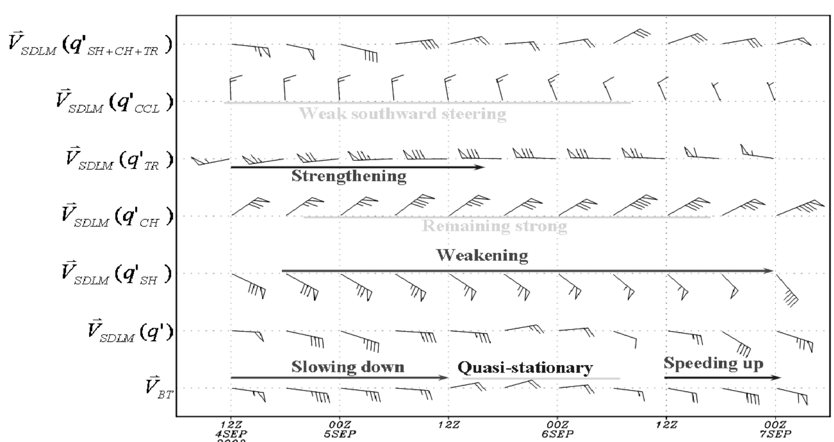

Figure 7. The time series of the movement of Sinlaku ($\vec{V}_{\mathrm{BT}}$) and the steering flow (averaged in the inner three latitude degrees between 975 and 300 hPa) associated with the total PV perturbation ($\vec{V}_{\mathrm{SDLM}}(q')$], and the PV perturbations of SH [$\vec{V}_{\mathrm{SDLM}}(q'_{\mathrm{SH}})$], CH [$\vec{V}_{\mathrm{SDLM}}(q'_{\mathrm{CH}})$], TR [$\vec{V}_{\mathrm{SDLM}}(q'_{\mathrm{TR}})$], and CCL [$\vec{V}_{\mathrm{SDLM}}(q'_{\mathrm{CCL}})$], individually. One full wind barb (a flag) represents 1 (5) ms^{-1}. (From Wu *et al.*, 2004.)

4. Targeted Observations and Data Assimilation for TC Motion (Wu *et al.* 2005, 2006, 2007a,b)

4.1. *Background*

Over the past 30 years, steady progress in the track forecasts of TCs has been made through the improvement of the numerical models, the data assimilation system, and the new data available to the forecast system (Wu, 2006). In addition to the large amount of satellite data, the special dropwindsonde data deployed from the surveillance aircraft have provided significant added value in improving the track forecasts.

In order to optimize the limited aircraft resources, targeted observations in the critical areas which have the maximum influence on numerical weather forecasts of TCs are of great importance. Therefore, targeted observing strategies for aircraft missions must be further developed. And it is a prerequisite for the device of observing strategy to identify the sensitive areas that have the greatest influence in improving the numerical forecast, or minimizing the track forecast error.

To make use of the available data or the potentially new data, it is important to evaluate the potential impact and to test the sensitivity of the simulation and prediction of TCs to different parameters. This understanding can be of great use in designing a cost-effective strategy for targeted observations of TCs (Morss *et al.*, 2001; Majumdar *et al.* 2002a,b; Aberson, 2003; Wu *et al.*, 2005).

In this section, three issues related to the author's works are addressed: (1) the impact of the DOTSTAR data; (2) results from a set of Observation System Simulation Experiments (OSSEs); (3) an innovative development of the new targeted observation strategy, the Adjoint-Derived Sensitivity Steering Vector (ADSSV).

4.2. *Impact of dropwindsonde data on TC track forecasts from DOTSTAR*

Since 2003, the research program of DOTSTAR (Wu *et al.*, 2005, 2007b) has continuously conducted dropwindsonde observations of typhoons in the western North Pacific (Fig. 8). Three operational global and two regional models were used to evaluate the impact of the dropwindsonde on TC track forecasting (Wu *et al.*, 2007b). Based on the results of 10 missions conducted in 2004 (Wu *et al.*, 2007b), the use of the dropwindsonde data from DOTSTAR has improved the 72 h ensemble forecast of three global models, i.e. the Global Forecasting System (GFS) of National Centers for Environmental Prediction (NCEP), the Navy Operational Global Atmospheric Prediction System (NOGAPS) of the Fleet Numerical Meteorology and Oceanography Center (FNMOC), and the Japanese Meteorological Agency (JMA), Global Spectral Model (GSM), by 22% (Fig. 9).

Wu *et al.* (2007b) showed that the average improvement of the dropwindsonde data made by DOTSTAR to the 72 h typhoon track prediction in the Geophysical Fluid Dynamics Laboratory (GFDL) hurricane models is an insignificant 3%. It is very likely that the signal of the dropwindsonde data is swamped by the bogusing procedure used during the initialization of the GFDL hurricane model. Chou and Wu (2007) showed a better way of appropriately combining the dropwindsonde data with the bogused vortex in the mesoscale model in order to further boost the effectiveness of dropwindsonde data with the implanted storm vortex.

4.3. *OSSE study (Wu et al., 2006)*

As the conventional observations usually have far less degrees of freedom than the models, the four-dimensional variational data assimilation

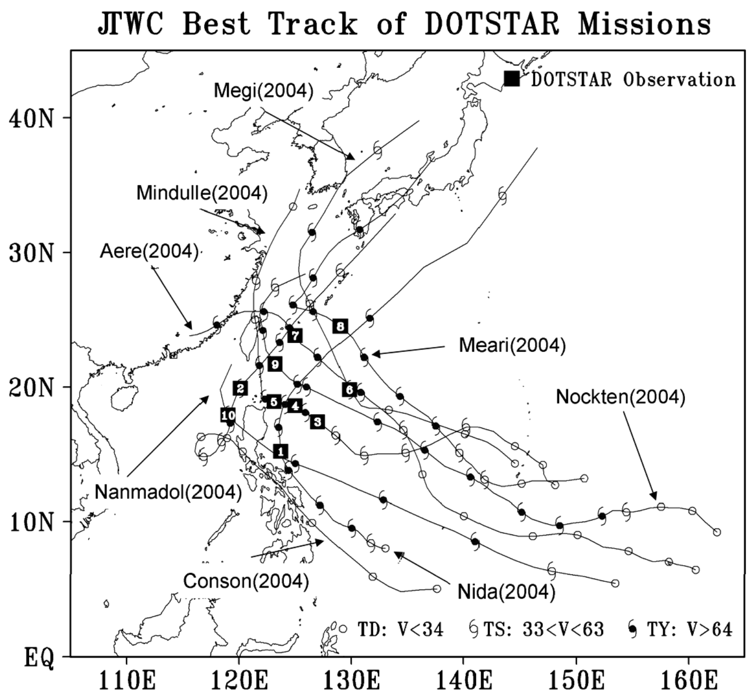

Figure 8. Best tracks (in typhoon symbols for every 24 h) of the eight typhoons with ten DOTSTAR observation missions in 2004. The squares indicate the storm locations where the DOTSTAR missions were taken. The numbers on the squares represent the sequence of the missions. (From Wu *et al.*, 2007b.)

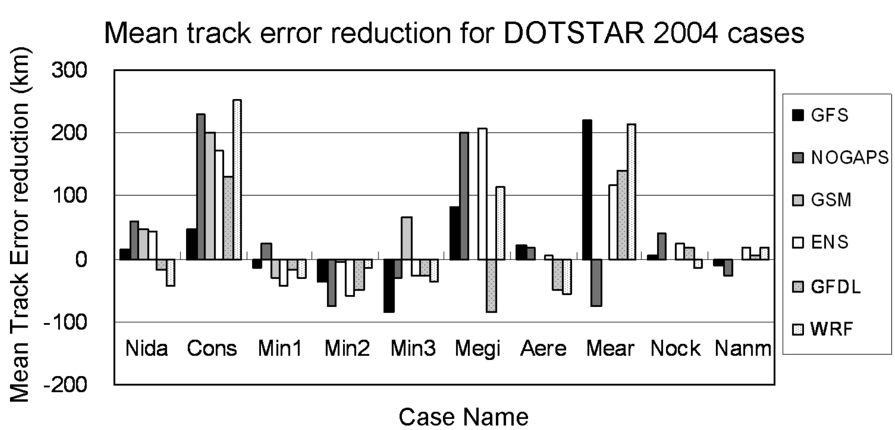

Figure 9. 6–72 h mean track error reduction (in km) after the assimilation of the dropwindsonde data into each of the ten models. The storm's name is abbreviated to the first four letters, while Min1, Min2, and Min3 stand for the first, second, and third cases in Mindulle. (From Wu *et al.*, 2007b.)

(4DVAR) has become one of the most advanced approaches to combining the observations with the model in such a way that the initial conditions are consistent with the model dynamics and physics (Guo *et al.*, 2000). Based on 4DVAR, a bogus data assimilation method has been developed by Zou and Xiao (2000) to improve the initial conditions for TC simulation.

A set of OSSEs have been performed to identify the critical parameters and the improved procedures for the initialization and prediction of TCs. A control experiment is carried out to create the imaginary "nature" data for Typhoon Zane (1996), using the fifth-generation Pennsylvania State University–National Center for Atmospheric Research Mesoscale Model (MM5). Then the initial data from the control experiment are degraded to produce the new initial condition and simulation, which mimics typical global analysis that resolves the Zane circulation. By assimilating some variables from the initial data of the control experiment into the degraded initial condition based on 4DVAR, the insight into the key parameters for improving the initial condition and prediction of TCs is attained (Wu *et al.*, 2006).

It is shown that the wind field is critical for maintaining a correct initial vortex structure of TCs. The model's memory of the pressure field is relatively short. Therefore, when only the surface pressure field is assimilated, due to the imbalance between the pressure and wind fields, the pressure field adjusts to the wind field and the minimal central sea-level pressure of the storm rises quickly.

It has been well demonstrated that taking the movement of the TC vortex into consideration during the data assimilation window can improve the track prediction, particularly in the early integration period. When the vortex movement tendency is taken into account during the bogus data assimilation period, it can partially correct the steering effect in the early prediction and the simulation period (Fig. 10). This concept provides a new and possible approach to the improvement of TC track prediction.

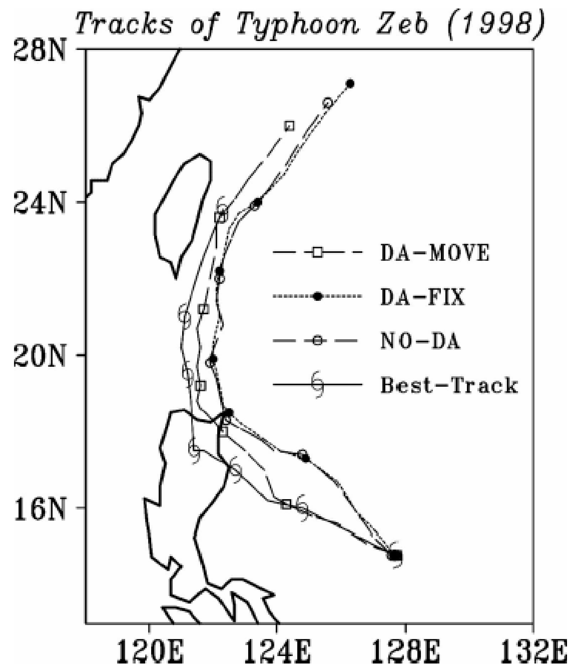

Figure 10. The 72 h JTWC best track (indicated with the typhoon symbol) and the simulated storm tracks from the experiments NO-DA, DA-FIX, and DA-MOVE for Typhoon Zeb (1998), shown for 12 h intervals from 0000 UTC, 13 October, to 0000 UTC, 16 October 1998. NO-DA: A standard MM5 simulation with an initial bogused vortex following Wu *et al.* (2002) without data assimilation. DA-FIX: An experiment assimilating the above bogused vortex (fixed in location) based on a 30-min-window 4DVAR data assimilation. DA-MOVE: An experiment in which the vortex is assimilated with the same initial data except that it moved in 3-h-window assimilation. (From Wu *et al.*, 2006.)

4.4. *Targeted observations for TCs (Wu et al., 2007a)*

(1) *Adjoint-Derived Sensitivity Steering Vector (ADSSV)*

By appropriately defining the response functions to represent the steering flow at the verifying time, a simple innovative vector, Adjoint-Derived Sensitivity Steering Vector (ADSSV), has been designed to clearly demonstrate the sensitive locations and the critical direction of the typhoon steering flow at the observing time.

Because the goal is to identify the sensitive areas at the observing time that will affect the steering flow of the typhoon at the verifying time, the response function is defined as the deep-layer-mean wind within the verifying area. A 600-km-by-600-km-square area centered on the MM5-simulated storm location is used to calculate the background steering flow as defined by Chan and Gray (1982), and two response functions are defined: R_1, the 850–300 hPa deep-layer area average (Wu *et al.*, 2003) of the zonal component (u), along with R_2, the average of the meridional component (v) of the wind vector, i.e.

$$R_1 \equiv \frac{\int_{850\,\mathrm{hPa}}^{300\,\mathrm{hPa}} \int_A u\ dxdydp}{\int_{850\,\mathrm{hPa}}^{300\,\mathrm{hPa}} \int_A dxdydp}, \tag{9}$$

$$R_2 \equiv \frac{\int_{850\,\mathrm{hPa}}^{300\,\mathrm{hPa}} \int_A v\ dxdydp}{\int_{850\,\mathrm{hPa}}^{300\,\mathrm{hPa}} \int_A dxdydp}. \tag{10}$$

By averaging, the axisymmetric component of the strong cyclonic flow around the storm center is removed, and thus the vector of (R_1, R_2) represents the background steering flow across the storm center at the verifying time. To interpret the physical meaning of the sensitivity, a unique new parameter, ADSSV, is designed to relate the sensitive areas at the observing time to the steering flow at the verifying time. The ADSSV with respect to the vorticity field (ς) is

$$\mathrm{ADSSV} \equiv \left(\frac{\partial R_1}{\partial \varsigma}, \frac{\partial R_2}{\partial \varsigma} \right), \tag{11}$$

where the magnitude of the ADSSV at a given point indicates the extent of the sensitivity, and the direction of the ADSSV represents the change in the response of the steering flow due to a vorticity perturbation placed at that point. For example, an increase in the vorticity at the observing time would be associated with an increase in the eastward steering of the storm at the verifying time, given that the ADSSV at one particular grid point aims toward the east at the forecast time.

The ADSSV, based on the MM5 forecast (Fig. 11), extends about 300–600 km from the north to the east of Typhoon Meari (2004). The directions of the ADSSVs indicate greater sensitivity in affecting the meridional component of the steering flow.

(2) *Recent techniques for targeted observations of TCs*
To optimize the aircraft surveillance observations using dropwindsondes, targeted observing strategies have been developed and examined. The primary consideration in devising such strategies is to identify the sensitive areas in which the assimilation of targeted observations is expected to have the greatest influence in improving the numerical forecast, or minimizing the forecast error. Since 2003, four objective methods have been tested for operational surveillance missions in the environment of Atlantic hurricanes conducted by National Oceanic and Atmospheric Administration (NOAA) (Aberson, 2003) and DOTSTAR (Wu *et al.*, 2005). These products are derived from four distinct techniques: the ensemble deep-layer mean (DLM) wind variance (Aberson, 2003), the ensemble transform Kalman filter (ETKF; Majumdar *et al.*, 2002), the total-energy singular vector (TESV) technique (Peng and Reynolds, 2006), and the Adjoint-Derived Sensitivity Steering Vector (ADSSV) (Wu *et al.*, 2007a). These techniques have been applied in a limited capacity to identify locations for aircraft-borne dropwinsondes to be collected in the environment of the TCs. For the surveillance missions in Atlantic hurricanes conducted by NOAA Hurricane Research Division (HRD; Aberson, 2003) and DOTSTAR (Wu *et al.*, 2005), besides the ADSSV method shown above, three other sensitivity techniques have been used to determine the observation strategies:

(i) *Deep-layer mean (DLM) wind variance*
Based on the DLM (850–200-hPa-averaged) steering flows from the NCEP Global Ensemble Forecasting System (EFS; Aberson, 2003), areas with the largest (DLM) wind ensemble spread represent the sensitive regions at the observing time. The DLM wind ensemble spread is chosen because TCs are generally steered by the environmental DLM flow, and the dropwindsondes from the NOAA Gulfstream IV sample this flow.

(ii) *Ensemble transform Kalman filter (ETKF)*
The ETKF (Bishop *et al.*, 2001) technique predicts the reduction in forecast error variance for a variety of feasible flight plans for deployment

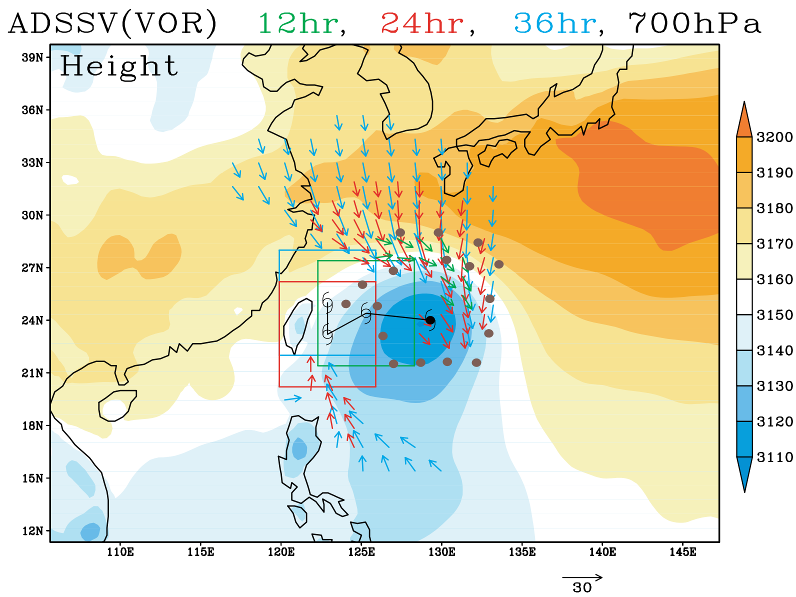

Figure 11. The ADSSV with respect to the vorticity field at 700 hPa with 12 h (in green), 24 h (in red), and 36 h (in blue) as the verifying time, superposed with the geopotential height field (magnitude scaled by the color bar to the right; the unit is m) at 700 hPa and the deployed locations of the dropsondes in DOTSTAR (brown dots). The scale of the ADSSV is indicated as the arrow to the lower right (unit: m). The 36 h model-predicted track of Meari is indicated with the typhoon symbol in red for every 12 h. The three square boxes represent the verifying areas at three different verifying times. (From Wu *et al.*, 2007a.)

of targeted observations based on the 40-member NCEP EFS (Majumdar *et al.*, 2006). That is, the ETKF uses the differences among ensemble members to estimate regions for observational missions. It takes the approach of DLM wind variance further. While DLM wind variance indicates areas of forecast uncertainty at the observation time, it does not correlate initial condition uncertainty with the errors in the forecasts. The ETKF explicitly correlates errors at the observation time with errors of the forecasts and identifies ensemble variance that impacts the forecasts in the verifying area at the verifying time.

(iii) Singular vector (SV) technique

The SV technique maximizes the growth of the total energy or kinetic energy norm (e.g. Palmer *et al.*, 1998; Peng and Reynolds, 2006) using the adjoint and forward-tangent models of the NOGAPS; Rosmond, 1997; Gelaro *et al.*, 2002), along with the ensemble prediction system (EPS) of the JMA and the SV products from European Center for Medium-Range Weather Forecasts (ECMWF). Peng and Reynolds (2006) have demonstrated the capability of the SV technique in identifying the sensitive regions suitable for targeted observations of TCs.

The above techniques have been applied in a limited capacity to identify locations for aircraft-borne dropwinsondes to be collected in the environment of the TCs. To gain more physical insights into these targeted techniques, studies to compare and evaluate the techniques have been conducted by Majumdar *et al.* (2006), Etherton *et al.* (2006), and Reynolds *et al.* (2007).

4.5. *Summary*

DOTSTAR, a TC surveillance program using dropwindsondes, has been successfully launched since 2003. To capture the sensitive areas which may influence the TC track, a newly designed vector, ADSSV, has been proposed (Wu *et al.*, 2007a). Aside from being used to conduct research on the impact of targeted observations, DOTSTAR's tropospheric soundings around the TC environment may also prove to be a unique dataset for the validation and calibration of remotely sensed data for TCs in the Northwest Pacific region.

Five models (four operational models and one research model) were used to evaluate the impact of dropwindsonde data on TC track forecasts during 2004. All models except the GFDL hurricane model show positive impacts from the dropwindsonde data on TC track forecasts. In the first 72 h, the mean track error reductions in the three operational global models, NCEP GFS, NOGAPS and JMA GSM, are 14%, 14%, and 19%, respectively, and the mean track error reduction of the ensemble of the three global models is 22%.

Along with the development of the ADSSV in DOTSTAR, an important issue on the targeted observations based on various techniques has been raised and should be further studied.

4.6. *Further thoughts (Wu, 2006)*

Experiments, such as the assimilation process of Numerical Weather Prediction (NWP) models conducted in recent years, have demonstrated their value in significantly reducing track forecast errors, suggesting that targeting observations are in need of more efforts. As reported at the 6th International Workshop on Tropical Cycones (Wu, 2006), some issues worth further exploration are:

(1) Research on targeted data should be extended to other observing systems and data (e.g. satellite-derived soundings). Application of new concepts in predictability and data assimilation should be tested.
(2) More studies of varying definitions, interpretations, and significance of sensitive regions (e.g. different methods, metrics) could be made.
(3) More work on metrics to assess the impact of targeting — or, more generally, on any changes in the observation network — should be done.
(4) Emphasis on the potential value of OSEs and OSSEs (e.g. Wu *et al.*, 2006) in assessing potential observing system impacts prior to actual field programs is needed.
(5) Stronger effort is needed to develop alternative observing platforms (other than the dropwindsondes) for targeting, especially adaptively selecting satellite observations by revising the data-thinning algorithms currently used.
(6) Improvement and continuous refinement of targeted observing strategies are required.
(7) The focus not only be on synoptic surveillance missions but also on inner core missions, especially in cyclone basins that have not been investigated yet.
(8) In addition to the targeted observations for TC motion, the targeting for TC intensity, structure, and rainfall prediction would be another challenging issue for further examination.

5. Concluding Remarks

Typhoons are the most catastrophic weather phenomenon in Taiwan, and ironically, the rainfall that typhoons bring is also a crucial water resource. Over the past 30 years, steady progress the motion of TCs has been well made through the improvement of the numerical models, the data assimilation and bogusing systems (Kurihara *et al.*, 1995; Xiao *et al.*, 2000; Zou and Xiao, 2000; Pu and Braun, 2001; Park and Zou, 2004; Wu *et al.*, 2006), the targeted observations (Aberson, 2003; Wu, 2006; Wu *et al.*, 2007a), and the new data available to the forecasting systems (Velden, 1997; Soden *et al.*, 2001; Zou *et al.*, 2001; Pu *et al.*, 2002; Zhu *et al.*, 2002; Chen *et al.*, 2004; Wu *et al.*, 2005, 2007b).

The author's perspective on the research works of TC motion has been presented in this article, and the major scientific contributions on TC motion issues from the author are summarized below:

(1) *The baroclinic effect on TC motion (Wu and Emanuel 1993, 1994)*
The dynamic properties of potential vorticity have been extensively utilized in observational work in meteorology. Potential vorticity concepts are first applied to the understanding of hurricane movement and hurricane structure, to a certain extent. Observations have shown that real TCs are strongly baroclinic, with broad anticyclones aloft. The interaction of the baroclinic hurricane vortex with background vertical shear may lead to storm drift, relative to the background mean flow, to the left (Northern Hemisphere) of the shear vector, and to a strong deformation of the outflow potential vorticity, resulting in jetlike outflow structure.

(2) *The potential vorticity perspective of the TC motion (Wu and Emanuel, 1995a,b; Wu and Kurihara, 1996; Wu et al., 2003, 2004)*
The potential vorticity diagnostics have been first designed to understand the controlling factors affecting the motion of typhoons. A newly proposed centroid-relative track, with the position weighting based on the steering flow induced by the PV anomaly associated with the other storm, has been plotted to highlight the binary interaction processes (Wu *et al.*, 2003). More detailed work has been conducted to evaluate and to quantify the physical factors that lead to the uncertainty of the typhoon movement, such as Sinlaku (2002) (Wu *et al.*, 2004). Further work is proposed to get into the physics of the statistical behavior of typhoon tracks in the whole of the western North Pacific region.

(3) *The targeted observations in improving TC motion (Wu* ***et al.****, 2005; Wu 2006; Wu et al., 2006, 2007a,b)*
As described by Wu and Kuo (1999, BAMS), the improvement of the understanding of typhoon dynamics and typhoon forecasting in the Taiwan area hinges very much on the ability to incorporate the available data into high-resolution numerical models through advanced data assimilation techniques. The considerable efforts with data assimilation research are shown in Wu *et al.* (2006), which demonstrates the wind field to be the most important key variable affecting the initialization and simulation of typhoons. In addition, to obtain sufficient typhoon data and to improve TC track forecasts, a pioneering research and surveillance program for TCs in the western North Pacific, DOTSTAR, has been conducted (Wu *et al.*, 2005). The flight routes enable observations in the most sensitive region around TCs, which is an area shown by several targeted observation methods, including the ADSSV, an innovative method developed by Wu *et al.* (2007a). It is believed that this adjoint sensitivity can be used to identify important areas and dynamical features affecting the TC track, and is helpful in constructing the strategy for adaptive observations. The ADSSV has been used among other methods for the targeted observations of typhoons in the western North Pacific (DOTSTAR) and hurricanes in the Atlantic (HRD's G-IV surverillance program).

Following the recommendation by Wu (2006), an intercomparison project has been initiated to evaluate the similarities and differences of all the different targeted techniques available. More analyses are ongoing to identify the similarities and differences of all these methods and to interpret their meaning dynamically. Results from this work would not only provide better insights into the physics of the targeted techniques, but also offer very useful information to assist future targeted observations. All this work is scheduled to be presented in a special selection on "Targeted Observation, Data Assimilation, and Tropical Cyclone Predictability" in the Monthly Weather Review of the American Meteorological Society.

Overall, DOTSTAR has had significant impact on the typhoon research and operation community in the international arena, and is also one of the key components of the newly developed project of T-PARC (THORPEX — Pacific Regional Campaign). Meanwhile, the Japanese team has also decided to conduct experiments (Typhoon Hunting 2008 — TH08) (T. Nakazawa, personal communication 2007) on targeted observations of TCs in 2008. It has been planned to fly two jets from both DOTSTAR and TH08 to target the same typhoon near the east of Taiwan and the south of Okinawa under T-PARC in 2008, so as to obtain the ideal and optimum dataset around the typhoon environment. With the potential international joint efforts of DOTSTAR and TH08 associated with T-PARC in 2008, the outlook for a further advance in the targeted observations and the predictability of the TC track is promising.

Acknowledgements

The author would like to thank all the collaborators for their contributions in the papers reviewed in this article. The helpful remarks of Yuqing Wang and another, anonymous reviewer are also appreciated. Special thanks also go to Prof. Po-Hsiung Lin and the COOK team on the DOTSTAR project, and the colleagues and students in my research group, "Typhoon Dynamics Research Center," at the Department of Atmospheric Sciences, National Taiwan University. The recent work is supported by the National Science Council of Taiwan through the grants NSC92-2119-M-002-009-AP1 and NSC93-2119-M-002-013-AP1, the Office of Naval Research grant N00014-05-1-0672, and MOTC-CWB-95-6M-03.

[Received 10 April 2007; Revised 13 September 2007; Accepted 17 September 2007.]

References

Aberson, S. D., 2003: Targeted observations to improve operational tropical cyclone track forecast guidance. *Mon. Wea. Rev.*, **131**, 1613–1628.

Bishop, C. H., and Z. Toth, 1999: Ensemble transformation and adaptive observations. *J. Atmos. Sci.*, **56**, 1748–1765.

Brand, S., 1970: Interaction of binary tropical cyclones of the western North Pacific Ocean. *J. Appl. Meteor.*, **9**, 433–441.

Carr, L. E., III, M. A. Boother, and R. L. Elsberry, 1997: Observational evidence for alternate modes of track-altering binary tropical cyclone scenarios. *Mon. Wea. Rev.*, **125**, 2094–2111.

Carr, L. E., III, and R. L. Elsberry, 1998: Objective diagnosis of binary tropical cyclone interactions for the Western North Pacific basin. *Mon. Wea. Rev.*, **126**, 1734–1740.

Chan, J. C.-L., and W. M. Gray, 1982: Tropical cyclone movement and surrounding flow relationship. *Mon. Wea. Rev.*, **110**, 1354–1376.

Chan, J. C.-L., 2005: The physics of tropical cyclone motion. *Annu. Rev. Fluid. Mech.*, **37**, 99–128.

Chen S.-H., F.C. Vandenberghe, G. W. Petty, and J. F. Bresch, 2004: Application of SSM/I satellite data to a hurricane simulation. *Quart. J. Roy. Meteor. Soc.*, **130**, 801–825.

Chang, S. W. J., 1983: A numerical study of the interaction between two tropical cyclones. *Mon. Wea. Rev.*, **112**, 1806–1817.

Chang, S. W. J., 1984: Reply. *Mon. Wea. Rev.*, **112**, 1646–1647.

Chou, K.-H., and C.-C. Wu, 2007: Development of the typhoon initialization in a mesoscale model — combination of the bogused vortex and the dropwindsonde data in DOTSTAR. *Mon. Wea. Rev.* (in press).

Davis, C. A., 1992: Piecewise potential vorticity inversion. *J. Atmos. Sci.*, **49**, 1397–1411.

DeMaria, M., and C. L. Chan, 1984: Comments on "A numerical study of the interactions between two tropical cyclones." *Mon. Wea. Rev.*, **112**, 1643–1645.

Dong, K., and C. J. Neumann, 1983: On the relative motion of binary tropical cyclones. *Mon. Wea. Rev.*, **111**, 945–953.

Dritschel, D. G., 1989: Contour dynamics and contour surgery: numerical algorithms for extended, high resolution modelling of vortex dynamics in two-dimensional inviscid compressible flows. *Computer Phys. Rep.*, **10**, 77–146.

Etherton, B., C.-C. Wu, S. J. Majumdar, and S. D. Aberson, 2006: A comparison of the targeting techniques for 2005 Atlantic tropical cyclones. Preprints, 27th Conf. on Hurricanes and Tropical Meteorology (Monterey, CA, USA, Amer. Meteor. Soc.).

Fiorino, M., and R. L. Elsberry, 1989: Some aspects of vortex structure related to tropical cyclone motion. *J. Atmos. Sci.*, **46**, 975–990.

Fujiwara, S., 1921: The mutual tendency towards symmetry of motion and its application as a principle in meteorology. *Quart. J. Roy. Meteor. Soc.*, **47**, 287–293.

Fujiwara, S., 1923: On the growth and decay of vortical systems. *Quart. J. Roy. Meteor. Soc.*, **49**, 75–104.

Fujiwara, S., 1931: Short note on the behavior of two vortices. *Proc. Phys. Math. Soc. Japan, Ser. 3*, **13**, 106–110.

Gelaro, R., T. E. Rosmond, and R. Daley, 2002: Singular vector calculations with an analysis error variance metric. *Mon. Wea. Rev.*, **130**, 1166–1186.

George, J. E., and W. M. Gray, 1976: Tropical cyclone motion and surrounding parameter relationships. *J. Appl. Meteor.*, **15**, 1252–1264.

Guo, Y.-R., Y.-H. Kuo, J. Dudhia, D. Parsons, and C. Rocken, 2000: Four-dimensional variational data assimilation of heterogeneous mesoscale observations for a strong convective case. *Mon. Wea. Rev.*, **128**, 619–643.

Holland, G. J., 1984: Tropical cyclone motion: a comparison of theory and observation. *J. Atmos. Sci.*, **41**, 68–75.

Holland, G. J., and G. S. Dietachmayer, 1993: On the interaction of tropical-cyclone-scale vortices. III: Continuous barotropic vortices. *Quart. J. Roy. Meteor. Soc.*, **119**, 1381–1398.

Hoskins, B. J., M. E. McIntyre, and A. W. Robertson, 1985: On the use and significance of isentropic potential-vorticity maps. *Quart. J. Roy. Meteor. Soc.*, **111**, 877–946.

Kurihara, Y., M. A. Bender, R. E. Tuleya, and R. J. Ross, 1995: Improvements in the GFDL hurricane prediction system. *Mon. Wea. Rev.*, **123**, 2791–2801.

Kurihara, Y., C. L. Kerr, R. E. Tuleya, and M. A. Bender, 1998: The GFDL hurricane prediction system and its performance in the 1995 hurricane season. *Mon. Wea. Rev.*, **126**, 1306–1322.

Lander, M., and G. J. Holland, 1993: On the interaction of tropical-cyclone-scale vortices. I: Observations. *Quart. J. Roy. Meteor. Soc.*, **119**, 1347–1361.

Majumdar, S. J., C. H. Bishop, R. Buizza, and R. Gelaro, 2002a: A comparison of ensemble-transform Kalman-filter targeting guidance with ECMWF and NRL total-energy singular-vector guidance. *Quart. J. Roy. Meteorol. Soc.*, **128**, 2527–2549.

Majumdar, S. J., C. H. Bishop, B. J. Etherton, and Z. Toth, 2002b: Adaptive sampling with the ensemble transform Kalman filter. Part II: Field program implementation. *Mon. Wea. Rev.*, **130**, 1356–1369.

Majumdar, S. J., S. D. Aberson, C. H. Bishop, R. Buizza, M. S. Peng, and C. A. Reynolds, 2006: A comparison of adaptive observing guidance for Atlantic tropical cyclones. *Mon. Wea. Rev.* (in press).

Molinari, J., 1993: Environmental controls on eye wall cycles and intensity change in Hurricane Allen (1980), in *Proc. ICSU/WMO Int. Symp. on Tropical Cyclone Disasters* (Beijing, China, World Meteorological Society) (Peking University Press), pp. 328–337.

Molinari, J., S. Skubis, and D. Vollaro, 1995: External influences on hurricane intensity. Part III: Potential vorticity structure. *J. Atmos. Sci.*, **52**, 3593–3606.

Montgomery, M. T., and B. F. Farrell, 1993: Tropical cyclone formation. *J. Atmos. Sci.*, **50**, 285–310.

Morss, R. E., K. A. Emanuel, and C. Snyder, 2001: Idealized adaptive observation strategy for improving numerical weather prediction. *J. Atmos. Sci.*, **58**, 210–232.

Palmer, T. N., R. Gelaro, J. Barkmeijer, and R. Buizza, 1998: Singular vectors, metrics, and adaptive observations. *J. Atmos. Sci.*, **55**, 633–653.

Park, K., and X. Zou, 2004: Toward developing an objective 4DVAR BDA scheme for hurricane initialization based on TPC observed parameters. *Mon. Wea. Rev.*, **132**, 2054–2069.

Peng, M. S., and C. A. Reynolds, 2006: Sensitivity of tropical cyclone forecasts. *J. Atmos. Sci.*, **63**, 2508–2528.

Pu, Z.-X., and S. A. Braun, 2001: Evaluation of bogus vortex techniques with four-dimensional variational data assimilation. *Mon. Wea. Rev.*, **129**, 2023–2039.

Pu, Z.-X., W.-K. Tao, S. Braun, J. Simpson, Y. Jia, H. Halverson, W. Olson, and A. Hou, 2002: The impact of TRMM data on mesoscale numerical simulation of Supertyphoon Paka. *Mon. Wea. Rev.*, **130**, 2448–2458.

Reynolds, C. A., M. S. Peng, S. J. Majumdar, S. D. Aberson, C. H. Bishop, and R. Buizza, 2007: Interpretation of adaptive observing guidance for Atlantic tropical cyclones. Submitted to *Mon. Wea. Rev.*

Ritchie, E. A., and G. J. Holland, 1993: On the interaction of tropical-cyclone-scale vortices. II: Discrete vortex patches. *Quart. J. Roy. Meteor. Soc.*, **119**, 1363–1379.

Rosmond, T. E., 1997: A technical description of the NRL adjoint model system. NRL/MR/7532/97/7230, Naval Research Laboratory, Monterey, CA, USA, 93943, 62 pp.

Ross, R. J., and Y. Kurihara, 1995: A numerical study of influences of Hurricane Gloria (1985) on the environment. *Mon. Wea. Rev.*, **123**, 332–346.

Shapiro, L. J., 1996: The motion of Hurricane Gloria: a potential vorticity diagnosis. *Mon. Wea. Rev.*, **124**, 1497–2508.

Shapiro, L. J., and J. L. Franklin, 1999: Potential vorticity asymmetries and tropical cyclone motion. *Mon. Wea. Rev.*, **127**, 124–131.

Soden, B. J., C. S. Velden, and R. E. Tuleya, 2001: The impact of satellite winds on experimental GFDL hurricane model forecasts. *Mon. Wea. Rev.*, **129**, 835–852.

Velden, C. S., C. M. Hayden, S. J. Nieman, W. P. Menzel, S. Wanzong, and J. S. Goerss, 1997: Upper-tropospheric winds derived from geostationary satellite water vapor observations. *Bull. Amer. Meteor. Soc.*, **78**, 173–195.

Wang Y., and G. J. Holland, 1995: On the interaction of tropical-cyclone-scale vortices. IV: Baroclinic vortices. *Quart. J. Roy. Meteor. Soc.*, **121**, 95–126.

Wang, B., R. Elsberry, and Y. Wang, 1998: Dynamics in tropical cyclone motion: a review. *Chinese J. Atmos. Sci.*, **22**, 416–434.

Wu, C.-C., and K. A. Emanuel, 1993: Interaction of a baroclinic vortex with background shear: application to hurricane movement. *J. Atmos. Sci.*, **50**, 62–76.

Wu, C.-C., and K. A. Emanuel, and 1994: On hurricane outflow structure. *J. Atmos. Sci.*, **51**, 1995–2003.

Wu, C.-C., and K. A. Emanuel, 1995a: Potential vorticity diagnostics of hurricane movement. Part I: A case study of Hurricane Bob (1991). *Mon. Wea. Rev.*, **123**, 69–92.

Wu, C.-C., and K. A. Emanuel, 1995b: Potential vorticity diagnostics of hurricane movement. Part II: Tropical Storm Ana (1991) and Hurricane Andrew (1992). *Mon. Wea. Rev.*, **123**, 93–109.

Wu, C.-C., and Y. Kurihara, 1996: A numerical study of the feedback mechanism of hurricane–environment interaction on hurricane movement from the potential vorticity perspective. *J. Atmos. Sci.*, **53**, 2264–2282.

Wu, C.-C., and Y.-H. Kuo, 1999: Typhoons affecting Taiwan: current understanding and future challenges. *Bull. Amer. Met. Soc.*, **80**, 67–80.

Wu, C.-C., T.-S. Huang, W.-P. Huang, and K.-H. Chou, 2003: A new look at the binary interaction: potential vorticity diagnosis of the unusual southward movement of Typhoon Bopha (2000) and its interaction with Typhoon Saomai (2000). *Mon. Wea. Rev.*, **131**, 1289–1300.

Wu, C.-C., T.-S. Huang, and K.-H. Chou, 2004: Potential vorticity diagnosis of the key factors affecting the motion of Typhoon Sinlaku (2002). *Mon. Wea. Rev.*, **132**, 2084–2093.

Wu, C.-C., P.-H. Lin, S. D. Aberson, T.-C. Yeh, W.-P. Huang, J.-S. Hong, G..-C. Lu, K.-C. Hsu, I.-I. Lin, K.-H. Chou, P.-L. Lin, and C.-H. Liu, 2005: Dropwindsonde observations for typhoon surveillance near the Taiwan Region (DOTSTAR): an overview. *Bull. Amer. Meteor. Soc.*, **86**, 787–790.

Wu, C.-C., 2006: Targeted observation and data assimilation for tropical cyclone track prediction. In *Proc. 6th Int. Workshop on Tropical Cyclones* (WMO/CAS//WWW, San Jose, Costa Rica, 21–28, Nov.), pp. 409–423.

Wu, C.-C., K.-H. Chou, Y. Wang, and Y.-H. Kuo, 2006: Tropical cyclone initialization and prediction based on four-dimension variational data assimilation. *J. Atmos. Sci.*, **63**, 2383–2395.

Wu, C.-C., J.-H. Chen, P.-H. Lin, and K.-H. Chou, 2007a: Targeted observations of tropical cyclone movement based on the Adjoint-Derived Sensitivity Steering Vector. *J. Atmos. Sci.*, **64**, 2611–2626.

Wu, C.-C., K.-H. Chou, P.-H. Lin, S. D. Aberson, M. S. Peng, and T. Nakazawa, 2007b: The impact of dropwindsonde data on typhoon track forecasts in DOTSTAR. *Wea. Forecasting*, **22**, 1157–1176.

Xiao, Q., X. Zou, and B. Wang. 2000: Initialization and simulation of a landfalling hurricane using a variational bogus data assimilation scheme. *Mon. Wea. Rev.*, **128**, 2252–2269.

Zhu, T., D.-L. Zhang, and F. Weng, 2002: Impact of the advanced microwave sounding unit measurements on hurricane prediction. *Mon. Wea. Rev.*, **130**, 2416–2432.

Zou, X., and Q. Xiao, 2000: Studies on the initialization and simulation of a mature hurricane using a variational bogus data assimilation scheme. *J. Atmos. Sci.*, **57**, 836–860.

Zou, X., Q. Xiao, A. E. Lipton, and G. D. Modica, 2001: A numerical study of the effect of GOES sounder cloud-cleared brightness temperatures on the prediction of Hurricane Felix. *J. Appl. Meteor.*, **40**, 34–55.